# Inhibition of vessel permeability by TNP-470 and its polymer conjugate, caplostatin

Ronit Satchi-Fainaro,[1] Roni Mamluk,[1] Ling Wang,[3] Sarah M. Short,[1] Janice A. Nagy,[2] Dian Feng,[2] Ann M. Dvorak,[2] Harold F. Dvorak,[2] Mark Puder,[1] Debabrata Mukhopadhyay,[2,3] and Judah Folkman[1,*]

[1]Children's Hospital Boston and Harvard Medical School, Vascular Biology Program, Department of Surgery, 1 Blackfan Circle, Karp Family Research Laboratories, Floor 12, Boston, Massachusetts 02115
[2]Department of Pathology, Beth Israel Deaconess Medical Center and Harvard Medical School, Boston, Massachusetts 02215
[3]Biochemistry and Molecular Biology and Mayo Cancer Center, Mayo Clinic, Rochester, Minnesota 55905
*Correspondence: judah.folkman@childrens.harvard.edu

## Summary

**Angiogenesis inhibitors, such as TNP-470 and the nontoxic HPMA copolymer-TNP-470 (caplostatin), are emerging as a class of anticancer drugs. We report that TNP-470 and caplostatin inhibit vascular hyperpermeability of tumor blood vessels as well as that induced in mouse skin by different mediators. Treatment with TNP-470 or angiostatin for 3 days was sufficient to reduce permeability of tumor blood vessels, delayed-type hypersensitivity, and pulmonary edema induced by IL-2. TNP-470 also inhibited VPF/VEGF-induced phosphorylation of VEGFR-2, calcium influx, and RhoA activation in endothelial cells. These results identify an activity of TNP-470, that of inhibiting vessel hyperpermeability. This activity likely contributes to TNP-470's antiangiogenic effect and suggests that caplostatin can be used in the treatment of cancer and inflammation.**

## Introduction

Angiogenesis, the generation of new blood vessels from preexisting microvasculature (Folkman and Kalluri, 2003), is regulated by a number of different growth factors (Matsumoto and Claesson-Welsh, 2001). Prominent among these is the vascular endothelial growth factor (VEGF) family of proteins (Neufeld et al., 1999). VEGF family members exert their activities by binding to three structurally related receptor tyrosine kinases, VEGF receptor (VEGFR)-1, -2, and -3. Neuropilins, heparan-sulfated proteoglycans, cadherins, and integrins serve as coreceptors for certain but not for all VEGF family proteins (Neufeld et al., 1999). VEGF-A exists in several different isoforms ($VEGF_{121}$, $VEGF_{165}$, $VEGF_{189}$), each of which has unique biological and biochemical properties (Feng et al., 2002). The most prominent VEGF-A isoform, $VEGF_{165}$, was initially discovered as a tumor-secreted protein that increased vascular permeability and was named vascular permeability factor (VPF) (Senger et al., 1983). Subsequently, VPF was shown to promote endothelial cell (EC) proliferation and migration and was renamed vascular endothelial growth factor (VEGF) (Ferrara and Henzel, 1989). As far as is known, $VEGF_{165}$, here referred to as VPF/VEGF, exerts most of its biological activities (EC proliferation, migration, survival, and permeability) by activating VEGFR-2 (Claesson-Welsh, 2003).

While EC proliferation is an important component of angiogenesis (Koch et al., 1994), VPF/VEGF has relatively weak mitogenic activity compared to other factors such as basic fibroblast growth factor (bFGF). However, VPF/VEGF is a potent vascular permeabilizing factor, and it has been known for some time that tumors and other forms of pathological angiogenesis are preceded and/or accompanied by enhanced vascular permeability (Dvorak, 2002; Folkman and Kalluri, 2003). In tumors that secrete VPF/VEGF, microvascular hyperpermeability results in extravasation of plasma and plasma proteins, leading to edema and deposition of an extravascular fibrin gel (Feng et al., 2000). This gel supports new blood vessel growth and the laying down of mature connective tissue stroma. Vascular hyperpermeability and fibrin deposition are also found in other examples of pathological angiogenesis mediated by VPF/VEGF, such as wound healing, arthritis, and psoriasis (Dvorak, 2002; Feng et al., 2000).

Given the prominence of vascular permeability in pathological angiogenesis, we investigated whether known angiogenesis inhibitors had an effect on vascular permeability. TNP-470, a synthetic analog of fumagillin, had been shown to block angi-

### SIGNIFICANCE

**It has long been known that the blood vessels supplying tumors and sites of inflammation are hyperpermeable to plasma and plasma proteins. Our study shows that several inhibitors of angiogenesis, TNP-470, its novel nontoxic polymeric conjugate caplostatin, and angiostatin, reduce plasma macromolecule extravasation from the pathologically hyperpermeable vasculature supplying tumors and inflammatory sites, and also from blood vessels rendered hyperpermeable by three vascular permeabilizing mediators, VEGF, PAF, and histamine. These inhibitors also reduced edema in tumors and pulmonary edema induced by IL-2 therapy and so could be useful as adjuvant therapy for tumors, inflammatory conditions, or complications of chemotherapy or immunotherapy. Our results describe a novel mechanism of action for TNP-470 and possibly other endogenous proteins with antiangiogenic activity.**

ogenesis (Ingber et al., 1990) and to inhibit tumor growth in several preclinical studies (Kragh et al., 1999) as well as in clinical trials (Milkowski and Weiss, 1999). TNP-470's clinical utility was limited by neurotoxicity, a complication that has recently been overcome by conjugating it to a water-soluble N-(2-hydroxypropyl)methacrylamide (HPMA) copolymer (Satchi-Fainaro et al., 2004). At present, the only known molecular target of TNP-470 is methionine aminopeptidase-2 (MetAP2) (Griffith et al., 1997), a cytoplasmic metalloenzyme responsible for removing the N-terminal methionine from nascent proteins. However, it is unclear how inhibition of this ubiquitously expressed protein affects TNP-470's action on EC proliferation (Ingber et al., 1990). To date, there is no evidence for TNP-470 binding an extracellular receptor.

TNP-470's effect on tumor growth has been thought to result mainly from its effects on EC proliferation (Abe et al., 1994). However, we demonstrate here that both TNP-470 and its nontoxic high-molecular weight HPMA copolymer conjugate, caplostatin, strikingly inhibit the vascular permeability-inducing effects of VPF/VEGF as well as that of platelet-activating factor (PAF) and histamine. TNP-470 inhibited extravasation of plasma proteins across microvascular endothelium in response to VPF/VEGF and other mediators in vivo as well as signaling pathways mediated through VEGFR-2, $Ca^{2+}$ influx, and RhoA activation on cultured endothelium. In addition, we show that TNP-470 inhibits the vascular hyperpermeability found in tumors and in delayed-type hypersensitivity (DTH) reactions, as well as in the pulmonary edema induced by interleukin-2 (IL-2). We also show that angiostatin, another angiogenesis inhibitor (O'Reilly et al., 1994), inhibits vascular permeability. Taken together, we demonstrate a mechanism by which TNP-470 and at least one other inhibitor antagonizes angiogenesis.

## Results

### TNP-470, caplostatin, and angiostatin reduce microvessel permeability

The Miles assay was used to determine whether TNP-470, caplostatin, or angiostatin affected vascular permeability, a prominent early feature of pathological angiogenesis (Figure 1). Evans blue dye was injected i.v., and immediately thereafter several vascular permeability-inducing agents (VPF/VEGF, PAF, histamine) were injected into the shaved flank skin of SCID mice. Evans blue dye binds to plasma proteins and therefore extravasates along with them at sites of increased permeability (Miles and Miles, 1952). VPF/VEGF-induced extravasation of Evans blue dye was strikingly inhibited (by ~70%) in mice treated for at least 24 hr with either TNP-470 or caplostatin (Figures 1A and 1B). Angiostatin treatment for 5 days also inhibited the vascular permeabilizing effects of VPF/VEGF but to a lesser extent (40%). In contrast, Herceptin and thalidomide, angiogenesis inhibitors that act indirectly on EC (Kerbel and Folkman, 2002), did not affect VPF/VEGF-induced vascular permeability (Figures 1A and 1B).

To determine whether the antipermeabilizing effects of TNP-470, caplostatin, and angiostatin were specific to VPF/VEGF, we tested their ability to inhibit the permeability-enhancing effects of PAF and histamine. TNP-470 and caplostatin reduced Evans blue dye accumulation induced by PAF and histamine by 75% and 80%, respectively; treatment with angiostatin reduced PAF- and histamine-induced permeability by 37% and 51%, respectively (Figure 1C). Of interest, TNP-470 and caplostatin also blocked the low-level permeability induced by intradermal injections of PBS (Figure 1C). These results indicate that angiogenesis inhibitors inhibit vascular permeability induced by mediators that are thought to act by different mechanisms and through different signaling pathways.

Comparisons of Miles assay results among different groups of animals are only valid if blood flow and volumes remain equivalent. To rule out the possibility that TNP-470's action on permeability was attributable to an effect on blood flow, we injected Evans blue dye i.v. into TNP-470-treated and untreated animals and collected skin samples 5 min later for dye

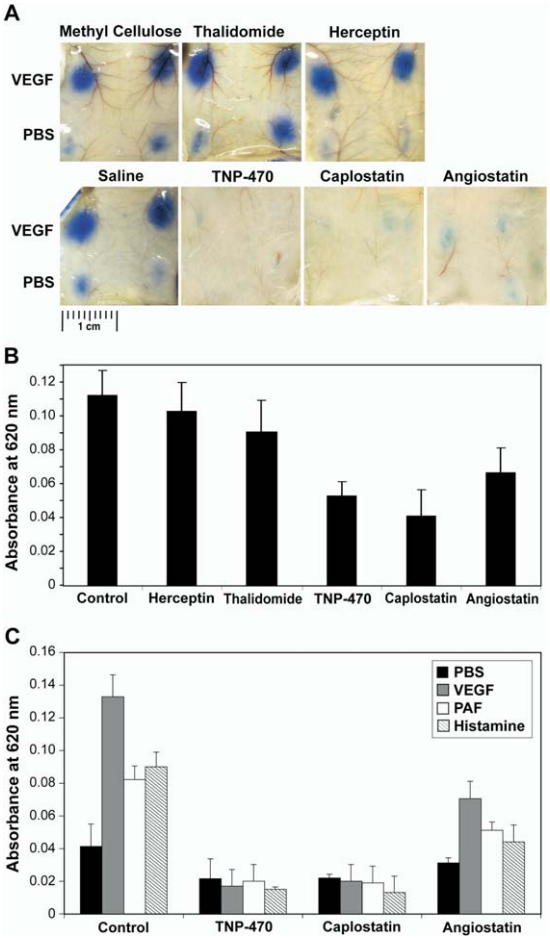


**Figure 1.** TNP-470 prevents vascular permeability in mouse skin capillaries

Vessel permeability was assessed by the Miles assay. Mice were pretreated systemically with saline, methyl cellulose, Herceptin, thalidomide, angiostatin, TNP-470, or caplostatin for 3–5 days and were then anesthetized and administered Evans blue i.v. (10 min) followed by intradermal injection of PBS (50 μl) and VPF/VEGF (50 ng in 50 μl) for 20 min.

**A:** Diminished dye is observed in mice treated with free or conjugated TNP-470 and angiostatin compared to treatment with thalidomide, Herceptin, or methyl cellulose and saline.

**B:** Skin was excised, and extracted dye contents were quantified by measuring at 620 nm. Data are expressed as mean ± SE.

**C:** Quantification of dye extracted from PBS (black columns)-, VEGF (gray columns)-, PAF (white columns)-, and histamine (striped columns)-induced permeability sites following treatments with TNP-470, caplostatin, angiostatin, or saline. Data are expressed as mean ± SE.

extraction. The rationale was that at 5 min after i.v. injection of Evans blue there is very little extravasation of dye, so the vast majority is contained within the blood vasculature; thus, extracted dye provides a measure of blood volume and flow (H. Zeng and H.F.D., unpublished data). We found no significant difference between control and TNP-470-treated groups (0.004 ± 0.0001 and 0.005 ± 0.0002, respectively). If TNP-470 had affected skin blood flow, for example, by constricting microvessels, we would have expected a reduction in Evans blue dye accumulation.

### TNP-470 decreases microvascular permeability in DTH reactions

DTH reactions are characterized by vascular hyperpermeability that is thought to be mediated by VPF/VEGF (Brown et al., 2000; Colvin and Dvorak, 1975). We therefore determined whether TNP-470 would also inhibit the edema characteristic of these reactions. DTH reactions in C57Bl/6J mice sensitized with oxazolone and treated with TNP-470 exhibited significantly reduced erythema and ear swelling as compared with control mice at 24 and 48 hr ($p < 0.01$; Figures 2A and 2B). No differences were found in the thickness of ears that were sensitized with the vehicle, but not challenged with oxazolone (Figure 2A). Histology confirmed the reduced swelling and showed that the inflammatory cell infiltrate was also reduced in TNP-470-treated mice (Figure 2C).

### TNP-470 decreases pulmonary edema induced by IL-2

Patients with metastatic renal cell carcinoma and malignant melanoma sometimes respond to IL- 2, but treatment with IL-2 is often limited by the development of systemic edema (Berthiaume et al., 1995). We therefore sought to determine whether TNP-470 could prevent this adverse side effect using an IL-2-induced pulmonary edema mouse model (Figure 3). As expected, IL-2-treated mice developed edematous lungs with wet weights 2.5× normal (419.4 ± 50.4 mg); also, histology revealed severe congestion and edema with intraalveolar fibrin deposits as well as perivascular and peribronchial mononuclear cell infiltrates. By contrast, the lungs of mice treated with TNP-470 remained normal in weight (170.2 ± 10.1 mg versus 177.8 ± 12.1 mg in control mice) and had normal histology. The improvement in lung edema could not be attributed to a generalized toxic effect of TNP-470, as over the 3 day period of treatment body weight did not decline.

### TNP-470 inhibits tumor blood vessel hyperpermeability

We next studied the effects of TNP-470 on tumor vessel permeability. We used six tumor cell lines whose expression of VPF/VEGF in vitro had been shown to differ widely and whose growth in vivo was inhibited to different extents (60%–95%) by TNP-470 (Figure 4A). Treatment with TNP-470 or caplostatin or with angiostatin in tumor-bearing mice inhibited Evans blue extravasation, but to different extents in different tumors: A2058 melanoma ($p < 0.03$ versus control), murine Lewis lung carcinoma (LLC) ($p < 0.05$), MCF-7 breast carcinoma ($p < 0.04$), MDA-MB-231 breast carcinoma ($p < 0.05$), and BXPC3 pancreatic adenocarcinoma ($p < 0.04$) by 40%–90% compared to control tumors treated with saline (Figure 4B). Interestingly, none of the drugs inhibited Evans blue extravasation into U87 glioblastomas (Figure 4B). A VPF/VEGF dose response was used in a modified Miles assay to test the effect of VEGF

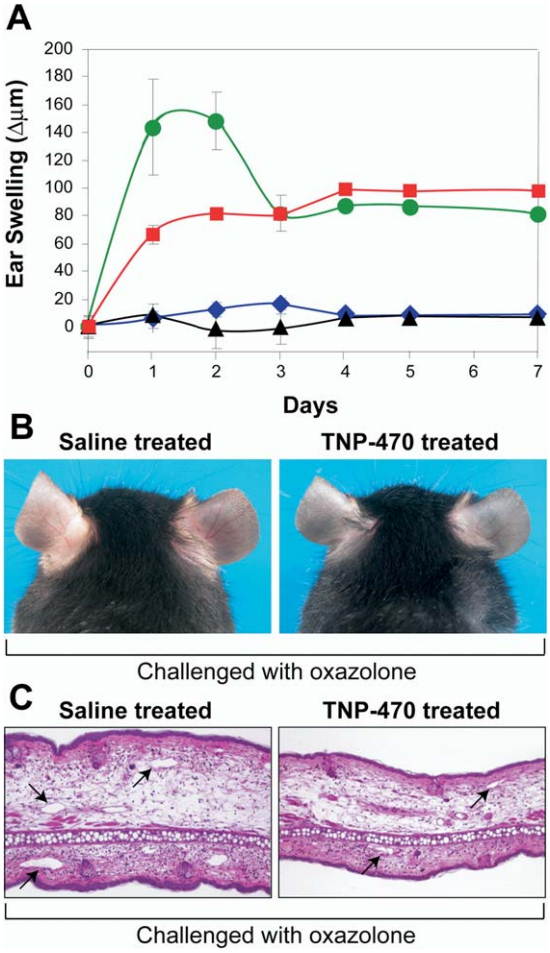


**Figure 2.** TNP-470 decreased ear swelling in DTH reactions elicited by oxazolone

DTH reactions were induced in the ear skin of C57Bl/6J mice using oxazolone challenge.

**A:** Ear swelling is expressed as the increase (Δμm) over the original ear thickness in micrometers. Mice treated with TNP-470 (red squares) showed a significantly decreased ear swelling ($p < 0.01$) 24 hr after challenge as compared with saline-injected challenged mice (green circles). Control left ears treated with vehicle alone in both groups showed no swelling (blue diamonds and black triangles). Data are expressed as mean ± SE.

**B:** Macroscopically visible increase of ear swelling and erythema in control mice (left panel) as compared with TNP-470-treated mice (right panel) at 24 hr after oxazolone challenge.

**C:** H&E staining shows increased extravasation of infiltrate into the extracellular matrix in control mice compared to TNP-470-treated mice, and arrows mark lymphatics (see arrows).

secreted from the tumor and the ability of TNP-470 to inhibit the permeability induced. Control saline-treated mice showed a dose-response correlation between increasing VPF/VEGF injection and dye accumulation, up to saturation (Figure 4C). TNP-470-treated mice showed inhibition of permeability up to 25 ng VPF/VEGF but, above that dose, TNP-470 lost its effectiveness in inhibiting permeability and dye accumulation (Figure 4C).

We also measured the levels of VPF/VEGF in U87 glioblastoma and A2058 melanoma tumor-bearing mice. VPF/VEGF levels in A2058 melanoma tumors were measured at 20 pg/100 mg and in U87 glioblastomas at 3192 ± 762 pg/100 mg.

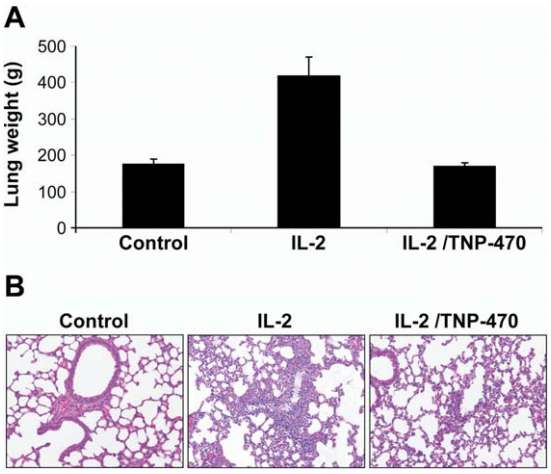


**Figure 3.** TNP-470 prevents IL-2-induced pulmonary edema

**A:** Mice were pretreated with saline or TNP-470 for 3 days and then injected with IL-2 for 5 days. Lungs from euthanized mice were dissected and weighed. Data are expressed as mean ± SE.

**B:** IL-2-induced pulmonary edema led to a massive thickening of the alveolar wall by extravasation of plasma proteins, generation of extracellular matrix, and cellular infiltration. Pretreatment with TNP-470 significantly reduced these effects.

Differences in vascular permeability could be affected by vessel number. Therefore, we determined whether TNP-470, caplostatin, or angiostatin had an effect on vessel density in mice implanted with the various tumor types. Following treatment with free or conjugated TNP-470 (for 3 days) or angiostatin (for 5 days), we found no significant difference in vessel density from control animals as determined by immunohistochemical staining for smooth muscle actin (SMA), proliferating cell nuclear antigen (PCNA), or CD31 staining in A2058 melanoma or U87 glioblastoma tumor models. CD31 staining of TNP-470, caplostatin, angiostatin, and untreated mice showed no difference in microvessel density in A2058 (76 ± 12, 90 ± 23, 65 ± 17, and 70 ± 14 microvessels/mm$^2$ ± standard error, respectively) or U87 glioblastoma (108 ± 24, 120 ± 13, 105 ± 15, and 118 ± 30 microvessels/mm$^2$ ± standard error, respectively). From this, we conclude that differences in permeability cannot be attributed to changes in vessel number or vessel density. Thus, the effect of TNP-470 on VPF/VEGF-induced permeability occurs without any effect on vessel number or density (vascular proliferation).

### TNP-470 does not affect the structure of vesiculo-vacuolar organelles or of interendothelial junctions

Plasma proteins have been reported to extravasate from the microvasculature by way of caveolae, fenestrae, and interendothelial cell gaps, and especially through vesiculo-vacuolar organelles (VVOs), a recently described structure in the endothelium of normal venules and of some tumor vessels (reviewed in Feng et al., 1996). Using transmission electron microscopy, we found that TNP-470 had no effect on microvascular structure (Figures 5A–5D). VVOs were normal with respect to frequency and size, interendothelial cell junctions were normally closed, and fenestrae remained rare. Intravenously administered ferritin extravasated from VPF/VEGF-injected sites via

A

| Tumor type | VEGF (pg/ml) (from conditioned media) | Inhibition of tumor growth by TNP-470 (%) | References |
|---|---|---|---|
| Lewis Lung Carcinoma | 113 | 67 | 1 |
| A2058 human melanoma | 120 | 65 | 1 |
| MCF-7 human breast cancer | 568 | 80 | 2 |
| MDA-MB-231 human breast cancer | 801 | 72 | 3 |
| BXPC3 human pancreatic adenocarcinoma | 1731 | 60 | 4 |
| U87 human glioblastoma | 40108 | 95 | 5 |

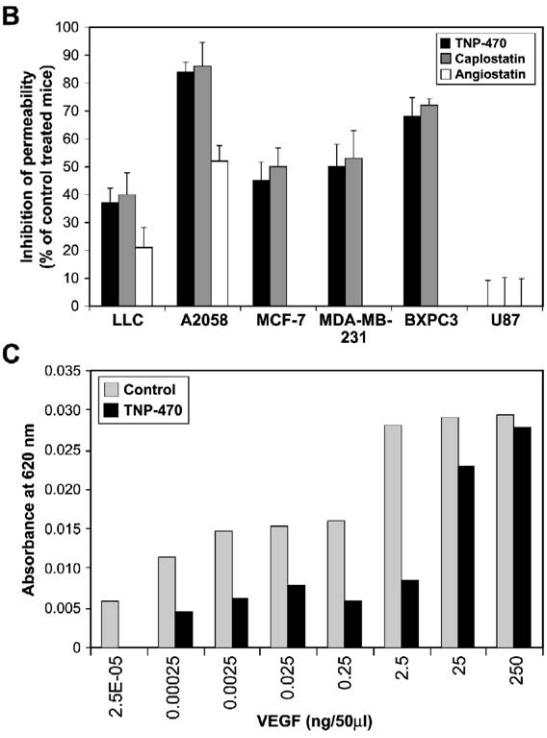


**Figure 4.** TNP-470 reduces tumor blood vessel permeability

**A:** VEGF levels in conditioned media of several cell lines. The growth of all tumors tested for permeability in **B** is known from the literature to be inhibited by TNP-470, as shown in the right column of the table. References are as follows: 1, Satchi-Fainaro et al. (2004); 2, McLeskey et al. (1996); 3, Yamaoka et al. (1993); 4, R.S.-F., A.E. Birsner, and J.F., unpublished data; 5, Takamiya et al. (1994).

**B:** Mice bearing LLC, A2058 melanoma, MCF-7 breast carcinoma, MDA-MB-231 breast carcinoma, BXPC3 pancreatic adenocarcinoma, or U87 glioblastoma were treated with saline (100%), TNP-470 (black columns), caplostatin (gray columns), or angiostatin (white columns; only LLC, A2058, and U87) for 3–5 days. Evans blue dye was injected, and after 10 min tumors were excised and weighed, and dye content per 100 mg tumor tissue was quantified at 620 nm. For each tumor, control group (saline) was determined as 100% permeability. Tumor vessel permeability was inhibited in all tumors except U87 glioblastoma. Data are expressed as mean ± SE.

**C:** C57Bl/6J mice were treated with TNP-470 (30 mg/kg/day s.c. for 3 days) or with saline and injected with Evans blue i.v. (10 min), followed by injection with VEGF intradermally at different concentrations. Skin punch biopsies were collected, and extracted dye in formamide was read at 620 nm. Control saline-treated mice showed a dose-response correlation between increasing VEGF injection and dye accumulation, up to saturation. TNP-470-treated mice showed inhibition of permeability up to 25 ng, but above that dose, TNP-470 lost its effectiveness in inhibiting permeability and dye accumulation.

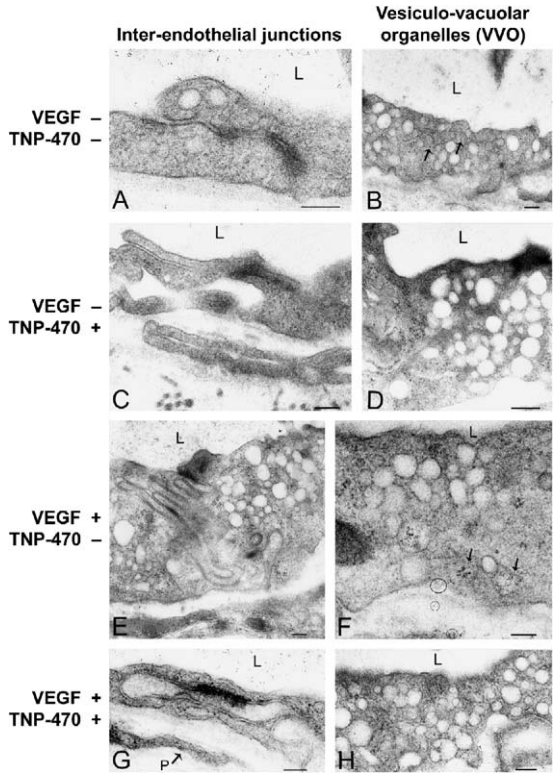


**Figure 5.** TNP-470 does not affect vesiculo-vacuolar organelle or endothelial junction structures

**A–D:** Venule EC in mice injected systemically with buffer (**A and B**) or TNP-470 (**C and D**). Interendothelial cell junctions (**A and C**) are normally closed, and vesiculo-vacuolar organelles (VVOs) are normal (**B and D**) in both sets of animals. There is minor leakage of intravenously injected circulating ferritin (**B**, small particles, some of which are in the lumen and the extravascular space) via VVOs (arrow marks a ferritin-containing vesicle). Leakage was reduced in the TNP-470-treated set (**C and D**).

**E–H:** Venule EC in mice injected locally with VPF/VEGF and systemically with buffer (**E and F**) or with TNP-470 (**G and H**). In both sets of mice, interendothelial cell junctions are normally closed (**E and G**), and VVOs are normal. Intravenously injected ferritin is seen to be extravasating through VVO vesicles (**F**, arrows) but to a lesser extent in TNP-470-treated mice (**G and H**). L, vascular lumen; p, pericyte. Scale bars, 200 nm.

VVOs as expected, and treatment with TNP-470 reduced such extravasation (Figures 5F and 5H). Small amounts of ferritin were also found in the VVOs of uninjected skin and in those of skin injected with buffer (Figure 5B) in untreated animals, and this was reduced in mice treated with TNP-470 (Figure 5D). Interendothelial cell junctions remained normally closed in all conditions tested. We conclude, therefore, that the antipermeability effect of TNP-470 is functional and not structural.

The effect of TNP-470 on interendothelial junction proteins was tested. Cultured bovine capillary EC (BCE) treated with or without TNP-470 (1 ng/ml) exhibited no differences in expression levels or distribution of occludin, claudin, ZO-1, β-catenin, and VE-cadherin (data not shown).

### TNP-470 inhibits VPF/VEGF-induced VEGFR-2 phosphorylation, EC proliferation, $Ca^{2+}$ influx, and MAPK phosphorylation

VPF/VEGF is thought to achieve its multiple effects on vascular endothelium primarily by activating VEGFR-2. We therefore investigated the effects of TNP-470 and caplostatin on the VEGFR-2 signaling pathway in cultured EC. TNP-470 reduced VPF/VEGF-induced phosphorylation of VEGFR-2 in human dermal microvascular endothelial cells (HMVEC-d) (Figure 6A) and human umbilical vascular endothelial cells (HUVEC) (Figure 6B) and did so at doses as low as 50 pg/ml (data not shown).

TNP-470 inhibited growth factor-induced proliferation of HMVEC-d at concentrations as low as 1 pg/ml without causing cytotoxicity (Figure 6C); only at concentrations above 1 μg/ml did TNP-470 become cytotoxic (below the basal cell proliferation in the absence of growth factors in the media). TNP-470 inhibited serum-induced proliferation (cytostatic effect) of U87 glioblastoma cells, but only at concentrations higher than 10 ng/ml (Figure 6C), and was only cytotoxic to tumor cells at concentrations higher than 100 μg/ml. Thus, TNP-470 inhibited VPF/VEGF-induced EC proliferation at concentrations four orders of magnitude below that required to inhibit tumor cell growth. This difference in sensitivity between tumor and endothelial cells has been extensively investigated previously with different cell lines (Milkowski and Weiss, 1999; Satchi-Fainaro et al., 2004).

TNP-470 and caplostatin also inhibited downstream signaling steps, including EC calcium influx ($[Ca^{2+}]_i$) (Figure 6D) necessary for vascular permeability and proliferation (D.M. and H.F.D., unpublished data), mitogen-activated protein kinase (MAPK) phosphorylation (Figure 6G), and RhoA activation (essential for VPF/VEGF-induced EC migration) (Figure 7).

Interestingly, TNP-470 and caplostatin also decreased $Ca^{2+}$ influx induced by histamine (Figure 6E) and by PAF (Figure 6F). These results suggest that TNP-470 does not inhibit permeability solely through inhibition of VEGFR-2 phosphorylation, because histamine and PAF act through different mechanisms.

### TNP-470 inhibits EC migration and RhoA activation

We next examined the effect of TNP-470 on VPF/VEGF-induced EC migration. Migration was assessed by counting the number of cells that migrated through the membranes toward the chemoattractant during a 4 hr period following 2 hr pretreatment with free or conjugated TNP-470 (1 ng/ml). Treatment with TNP-470 or caplostatin dramatically inhibited the chemotactic migration response to VPF/VEGF by 68% ($p = 0.00045$) and 87% ($p = 0.000096$), respectively (Figure 7A). In contrast, cells treated with HPMA copolymer alone (at 1 μg/ml TNP-470-equivalent concentration) migrated similarly to untreated control HMVEC-d. TNP-470 also inhibited basal migration of HMVEC-d cells in the absence of VPF/VEGF by 70% ($p = 0.0023$).

The RhoA superfamily of small GTPase has been shown to play a key role in cell proliferation, shape change, and migration (Aspenstrom, 1999). RhoA and Rac1 are required for VEGFR-2-mediated HMVEC-d migration (Zeng et al., 2002). Therefore, we examined the possible role of RhoA in TNP-470's inhibition of VPF/VEGF-mediated HMVEC-d migration. VPF/VEGF induced RhoA activation in HMVEC-d. TNP-470 significantly decreased VPF/VEGF-activated RhoA (Figure 7B; densitometrical quantification shown on the figure). These results suggest that RhoA inhibition by TNP-470, at least in part, leads to the inhibition of VPF/VEGF-induced migration of HMVEC-d. We also tested the effect of TNP-470 on PAF-induced (Figure 7C) and histamine-induced (Figure 7D) RhoA activation, and these were inhibited by TNP-470 and caplostatin as well.

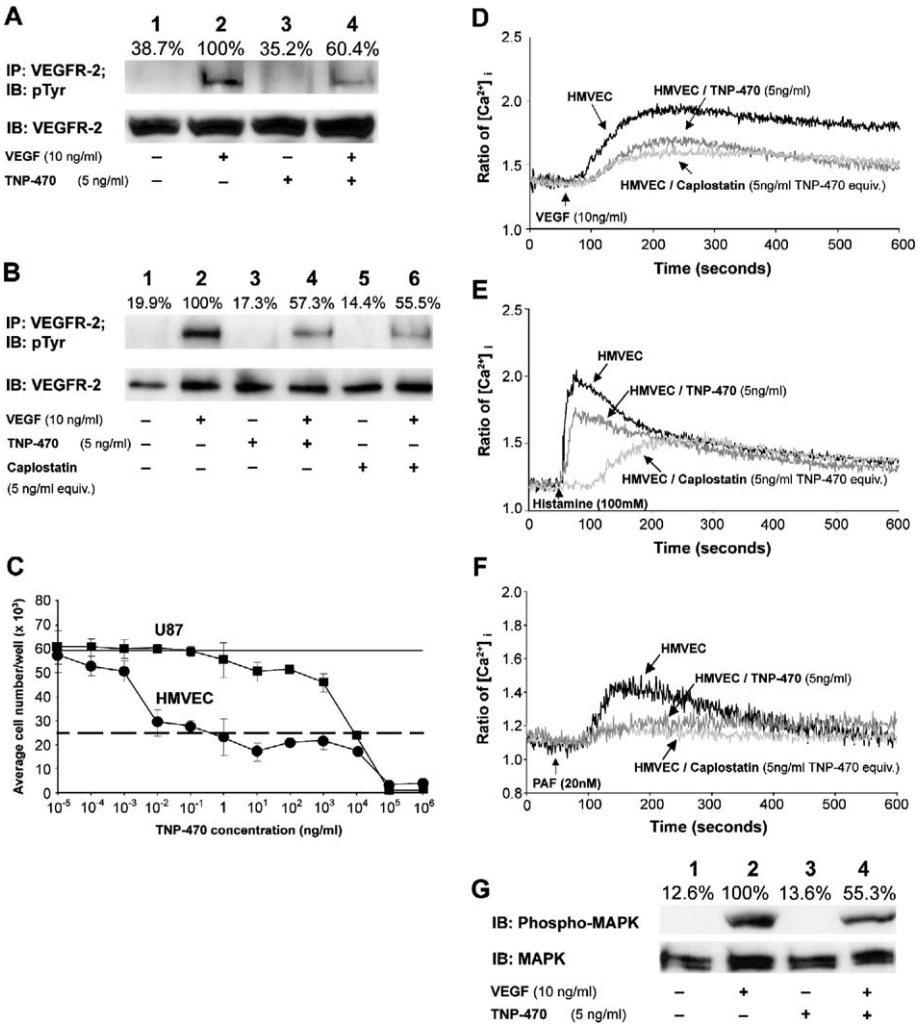


**Figure 6.** Free and conjugated TNP-470 inhibit VPF/VEGF-induced VEGFR-2 phosphorylation, EC proliferation, $Ca^{2+}$ influx, and MAPK in vitro

**A and B:** TNP-470 inhibits VEGFR-2 phosphorylation in HMVEC-d (**A**) and HUVEC (**B**). This Western blot is representative of five experiments. Inhibition of VEGFR-2 phosphorylation ranged between 10% and 40%.

**C:** TNP-470 inhibited U87 glioblastoma (black squares) and HMVEC-d (black circles) proliferation after 72 hr. The solid line represents the proliferation of growth factor-induced cells, and the dotted line represents cell proliferation in the absence of growth factors. Data are expressed as mean ± SE.

**D–F:** $Ca^{2+}$ influx in HMVEC-d induced by VEGF (**D**), histmanine (**E**), or PAF (**F**) following treatment with TNP-470 or caplostatin was reduced compared to control.

**G:** TNP-470 inhibits VPF/VEGF-induced MAPK phosphorylation in HMVEC-d. Densitometrical analysis is presented as percentage of band intensity compared to VEGF-stimulated control.

To determine whether VPF/VEGF-induced permeability was mediated by the RhoA pathway, we used Y27632, a pharmacological inhibitor of Rock, a downstream target of RhoA (Breslin and Yuan, 2004). Rock is a kinase that has been implicated in the formation of cell-cell junctions. Pretreatment of SCID mice with Y27632 inhibited VPF/VEGF-induced and *Escherichia coli* cytotoxic necrotizing factor-1 (CNF-1)-induced Evans blue-albumin extravasation (Figure 7E). Activation of RhoA with CNF-1 (Hopkins et al., 2003) was sufficient to promote extravasation, because CNF-1 induced vessel leakage in the Miles assay when injected intradermally (Figures 7E and 7F). This response was inhibited by Y27632; thus, RhoA pathway appeared to be a key mediator of VPF/VEGF-induced leakage. Pretreatment of SCID mice with TNP-470 also inhibited CNF-1-induced Evans blue-albumin extravasation (Figures 7E and 7F). These results suggest that systemic in vivo inhibition of RhoA causes inhibition of VPF/VEGF-induced vessel leakiness and that TNP-470 inhibits vessel permeability through inhibition of RhoA activation.

## Discussion

Tumor growth beyond a minimal size requires the generation of new blood vessels, and for this reason recent attention has been paid to antiangiogenesis as an approach to tumor therapy. Tumors induce their new blood vessels by secreting angiogenic cytokines, of which VPF/VEGF is arguably the most important. Some antiangiogenic agents have well-defined targets, such as antibodies against VEGF or kinase inhibitors directed against VEGF receptors (Kerbel and Folkman, 2002). However, little is known about the mechanism of action of other angiogenesis inhibitors, including TNP-470, caplostatin, and angiostatin, that act directly on vascular endothelium. The present study was designed to determine whether these inhibitors affected steps in the angiogenic cascade other than EC proliferation and to begin to define their molecular targets. We report here that TNP-470, caplostatin, and angiostatin act, at least in part, by inhibiting vascular permeability and EC migration, both intrinsic properties of pathological angiogenesis. We also report initial studies that identify steps in the VPF/VEGF signaling cascade that are affected by these agents.

Angiogenesis is a complex process that involves EC division, migration, acquisition of pericytes, and other organizational steps, not all of which have been defined. In addition, all forms of pathological angiogenesis thus far identified are characterized by vascular hyperpermeability, a state thought to result from the expression of VPF/VEGF (Carmeliet and Collen, 2000;

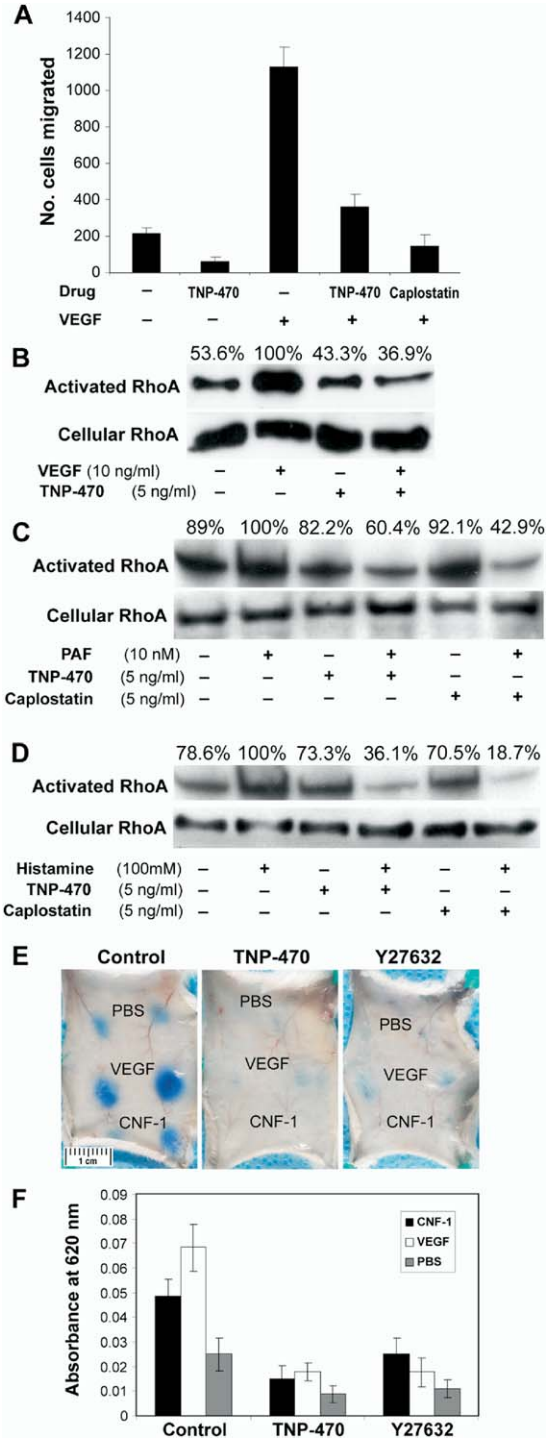


**Figure 7.** Effect of VPF/VEGF and RhoA signaling on HMVEC migration in vitro and on vessel permeability in vivo

**A:** HMVEC-d migration to VPF/VEGF. TNP-470 and caplostatin inhibited basal and VPF/VEGF-induced migration of HMVEC-d. Data are expressed as mean ± SD.

**B–D:** TNP-470 and caplostatin inhibited RhoA activation in HMVEC-d induced by VPF/VEGF (**B**), PAF (**C**), or histamine (**D**). Densitometrical analysis is presented as percentage of band intensity compared to VEGF-stimulated control.

**E:** TNP-470 and Y27632 inhibited both VPF/VEGF- and CNF-1-induced vessel permeability.

Matsumoto and Claesson-Welsh, 2001). Whether in tumors, inflammation, or wound healing, vascular hyperpermeability results in edema, clotting, and deposition of an extravascular fibrin gel that provides a provisional matrix that favors angiogenesis and mature stroma generation. Vascular hyperpermeability also contributes to morbidity caused by inducing fluid accumulation in body cavities (e.g., pleural and peritoneal cavities) and in the brain, where edema can become a life-threatening complication (Ohnishi et al., 1990). Recently, prevention of microvascular permeability by endothelial nitric oxide synthase (eNOS) inhibition (see below) has been successfully exploited as an approach to tumor therapy (Gratton et al., 2003).

Given this background, we set out to determine whether the potent angiogenesis inhibitors TNP-470, caplostatin, and angiostatin had an effect on vascular permeability in tumors and other examples of pathological angiogenesis. All six of the tumors studied exhibited increased permeability, and we demonstrated that TNP-470, caplostatin, and angiostatin effectively inhibited the permeability response in five tumors. The lone exception was the U87 glioblastoma, a tumor that secretes unusually large amounts of VPF/VEGF. This finding might be explained by the dose-response data that show a threshold above which TNP-470 is not able to inhibit VPF/VEGF-induced permeability, at least under the conditions of our experiments. Nonetheless, TNP-470 did inhibit the growth of the U87 tumor, indicating that factors other than its antipermeability action contribute to TNP-470's effectiveness in preventing tumor growth. TNP-470 was also effective in inhibiting the vascular permeability characteristic of delayed hypersensitivity reactions, which, like that of tumors, is thought to result from VPF/VEGF expression.

Other experiments were performed to determine whether the action of TNP-470 and angiostatin was specific for VPF/VEGF-induced vascular permeability. We demonstrated that treatment of mice with TNP-470 for as little as 24 hr suppressed not only the permeability response to VPF/VEGF but also that to PAF and histamine. We also demonstrated that animals treated with TNP-470 were protected from the pulmonary edema induced by IL-2. Taken together, these data indicate that TNP-470, caplostatin, and angiostatin inhibit the vascular permeability responses induced by a variety of agonists that have been thought to act in different ways and by different signaling pathways. Endostatin (M. Nomi, G. Schuch, N. Kilic, L. Oliveira-Ferrer, R.S.-F., J. Weil, D.K.H., A. Atala, J.F., S. Soker, and S. Ergun, personal communication) and endostatin peptides (Tjin Tham Sjin et al., 2005) also inhibit vascular permeability. It is possible, therefore, that these agents, and particularly TNP-470 in its nontoxic polymeric form, will be of therapeutic value not only in tumors but also in other circumstances where vascular permeability is a problem, e.g., inflammatory and hypersensitivity disorders, treatments with IL-2, cerebral edema resulting from stroke, lymphedema, etc.

Although TNP-470 decreased permeability, our examination

**F:** Quantification of dye content in skin areas of the extravasation of Evans blue dye at injection sites. TNP-470 and Y27632 reduced both VPF/VEGF- and CNF-1-induced vessel permeability to Evans blue-albumin complex. Data are expressed as mean ± SE.

of EC structure showed that VVOs were found to be normal in number and extent, interendothelial cell junctions appeared to be normal, and fenestrae were not detectably increased in TNP-470-treated animals. These data indicate that TNP-470 affects EC function but not structure. Consistent with these results, we found no changes in junctional proteins of cultured EC that were treated with TNP-470.

In addition to inhibiting vascular permeability and EC proliferation, TNP-470 also inhibited VPF/VEGF-induced EC migration. Recent work has done much to elucidate the signaling steps by which VPF/VEGF mediates its several effects, and we therefore sought to define the signaling events that were inhibited by TNP-470. We found that TNP-470 inhibited VEGFR-2 phosphorylation as well as such downstream signaling steps as MAPK phosphorylation and calcium influx. TNP-470 also reduced VPF/VEGF-induced RhoA activation. RhoA is a major player in cytoskeleton organization and in cellular tension generation (Hall, 1998; Ingber, 2002) and has an important role in both EC proliferation and migration. Further, it has been suggested that RhoA activation triggers $Ca^{2+}$ entry via intracellular store depletion, a precursor step to endothelial permeability (Mehta et al., 2003). It has long been known that VPF/VEGF stimulates transient accumulation of cytoplasmic calcium in cultured EC (Brock et al., 1991). The increases in endothelial cytosolic $Ca^{2+}$ induced by VPF/VEGF, and also by PAF and histamine, likely activate calcium/calmodulin-dependent enzymes such as eNOS. It has been previously shown that TNP-470 inhibits nitric oxide production (Mauriz et al., 2003), and nitric oxide has been implicated in VPF/VEGF-driven vascular permeability (Fukumura et al., 2001). Activation of eNOS by VPF/VEGF involves several pathways, including Akt/PKB, calcium/calmodulin, and protein kinase C (Aoyagi et al., 2003; Aramoto et al., 2004). Taking all of these facts together, we have proposed in Figure 8 a model by which TNP-470 may act as an antipermeability factor.

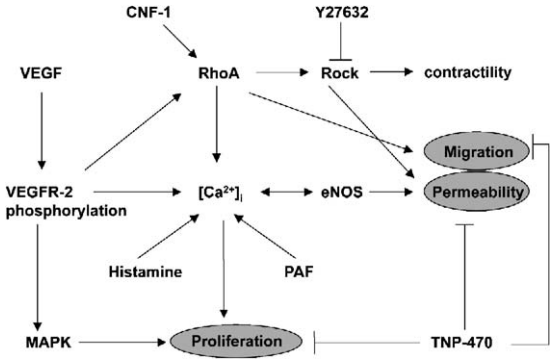


**Figure 8.** Schematic model for proposed mechanism of TNP-470 inhibition of vessel permeability

TNP-470 inhibits migration and proliferation of EC and prevents VEGF-, PAF-, and histamine-induced permeability. VEGF, PAF, and histamine enhance vascular leakage by opening of interendothelial junctions, endothelial fenestration, generation of transendothelial gaps, and transcytotic vesicles including VVO. Pretreatment with TNP-470 decreases the leakage via transcytotic vesicles. TNP-470 inhibited VEGFR-2 phosphorylation, $[Ca^{2+}]_i$, and RhoA activation in vascular endothelium. This model suggests that TNP-470 transforms angiogenic and hyperpermeable vessels to a less leaky morphologic phenotype.

## Experimental procedures

### Materials

TNP-470 was kindly provided by Takeda Chemical Industries Ltd. (Japan). HPMA copolymer precursor was from Polymer Laboratories (UK). Caplostatin was synthesized as previously described (Satchi-Fainaro et al., 2004). $VEGF_{165}$ was a gift from the NIH (Bethesda, CA). Bovine serum albumin (BSA), dimethylformamide (DMF), formamide, Evans blue, histamine, and oxazolone (4-Ethoxymethylene-2-phenyloxazolone) were from Sigma (St. Louis, MO). PAF was from Biomol (Plymouth Meeting, PA), Vivacell 70 ml dialysis system (10 kDa MW cutoff PES) was from VivaScience (USA). Isoflurane was purchased from Baxter Healthcare Corporation (USA). Matrigel was from Becton Dickinson (USA), Avertin was from Fisher (USA), and thalidomide was from Celgene (USA). Human and mouse VPF/VEGF quantikine ELISA kits were purchased from R&D Systems Inc. (Minneapolis, MN). Angiostatin was from EntreMed (USA), anti-Erb B-2 antibody (Herceptin) was from Genentech (USA), and IL-2 was a gift from Dr. Steven A. Rosenberg (NIH). Rabbit polyclonal antibody against RhoA, anti-Flk-1 mouse monoclonal, and an antibody against phosphorylated tyrosine (*pTyr*) mouse monoclonal were purchased from Santa Cruz Biotechnology (Santa Cruz, CA). Anti-Phospho-p44/42 MAPK mouse monoclonal antibody and anti-p44/42 MAPK rabbit polyclonal antibody were from Cell Signaling Technology, Inc. Y27632 was from Calbiochem (San Diego, CA). His-CNF1 plasmid was a gift from Melody Mills (Uniformed Services University of Health Sciences, MD) and was expressed in *Escherichia coli*; recombinant CNF-1 was purified with the QIAGEN kit. Glutathione-S-transferase (GST)-Rhotekin Rho binding domain (TRBD) fusion protein was provided by Dr. Martin Schwartz (Scripps Institute) (Ren et al., 1999).

### Cell culture

Tumor cells (A2058 human melanoma, U87 human glioblastoma, BXPC3, LLC, MCF-7, MDA-MB-231) were obtained from the American Type Culture Collection (Manassas, VA). Cells were cultured as previously described (Satchi-Fainaro et al., 2004). BCE cells were isolated and maintained as described (Folkman et al., 1979). HMVEC-d and HUVEC were obtained from Cambrex (Walkersville, MD) and grown according to the manufacturer's protocol in EGM-2 MV medium or EGM, respectively, supplemented with bullet kits (Cambrex).

### Mice

C57Bl/6J mice were purchased from Jackson Laboratories (USA), and CB-17 SCID mice were purchased from Massachusetts General Hospital (USA). All animal procedures were performed in compliance with Boston Children's Hospital guidelines and protocols approved by the Institutional Animal Care and Use Committee.

### Miles vascular permeability assay

SCID mice were injected subcutaneously (s.c.) with TNP-470 or caplostatin (30 mg/kg TNP-470-equivalent concentration) for 3 days, with Y27632 (50 nM s.c.) for 11 days, with angiostatin (200 mg/kg/day s.c.) for 5 days, or with saline (250 μl s.c.) for 5 days (n = 12 mice/group) before the Miles assay was performed (Claffey et al., 1996; Miles and Miles, 1952; Streit et al., 2000). Briefly, Evans blue dye (100 μl of a 1% solution in 0.9% NaCl) was injected intravenously (i.v.) into mice. After 10 min, 50 μl of human $VEGF_{165}$ (1 ng/μl), PAF (100 μM), CNF-1 (100 ng), histamine (1.2 μg/ml), or PBS was injected intradermally into the preshaved back skin. After 20 min, the animals were euthanized, and an area of skin that included the entire injection site was removed. Evans blue dye was extracted from the skin by incubation with formamide for 5 days at room temperature, and the absorbance of extracted dye was measured at 620 nm. In addition, in order to test the effect of TNP-470 on blood volume and flow we measured dye accumulation in the uninjected flank skin of mice treated as above with TNP-470 or saline. Five minutes later, we performed punch biopsies of flank skin from both sets of mice and extracted these with formamide as above. The unpaired Student's t test was used for statistical analysis.

### Tissue processing for electron microscopy

SCID mice were treated for 3 days with TNP-470 or saline as above, following which anionic ferritin was injected as tracer i.v.; 50 μl of human $VEGF_{165}$

(1 ng/μl) or 50 μl of PBS was then injected i.d. into preshaved flank skin. After 15 min, animals were euthanized. Skin test and control sites were excised and fixed by immersion and processed for electron microscopy as previously described (Dvorak et al., 1996; Feng et al., 1996).

**Endothelial junctional proteins**

BCE were cultured on glass coverslips in a 24-well plate (200,000 cells/well) in Dulbecco's modified Eagle's medium (DMEM) + 10% bovine calf serum (BCS) + 3 ng/ml bFGF in the presence or absence of TNP-470 (1 ng/ml) for 3 days. Thereafter, PAF (100 μM) or VEGF (50 ng/ml) was added for 20 min, and the cells were fixed in paraformaldehyde 4% for 10 min and in methanol for 5 min at room temperature. Fixed cells were incubated overnight with polyclonal antibodies to occludin, claudin, ZO-1, or VE-cadherin or a monoclonal antibody to β-catenin (Zymed Laboratories, South San Francisco, CA). The staining was subsequently developed with FITC-conjugated secondary antibodies and photographed using a fluorescent microscope.

**DTH reactions**

DTH reactions were induced in the flank skin of 8-week-old C57Bl/6J male mice (n = 5) as previously described (Dvorak et al., 1984). Mice were sensitized by topical application of 2% oxazolone solution in vehicle (acetone:olive oil, 4:1 vol/vol), to the shaved abdomen (50 μl) and to each paw (5 μl). Mice were treated with TNP-470 (30 mg/kg s.c.) for 3 days beginning on day 2, and at 5 days the right ears were challenged by topical application of 10 μl of a 1% oxazolone solution; the left ears were treated with vehicle alone. Ear thickness was then measured daily for 7 days as a measure of inflammation intensity (Gad et al., 1986). Statistical analysis was performed using the unpaired Student's t test. Some mice from each experimental group were euthanized 24 hr after oxazolone challenge (n = 5 per group). One half of each ear was fixed in 10% formalin and processed for H&E-stained paraffin sections. The other half was embedded in OCT compound (Sakura Finetek, Torrance, CA) and snap frozen in liquid nitrogen for immunohistochemical staining of 5 μm cryostat sections using a Vecstatin avidin-biotin detection system (Vector Labs, Burlingame, CA) with rat monoclonal antibodies against mouse CD31 (dilution 1:250; Pharmingen, San Diego, CA).

**IL-2-associated pulmonary edema**

C57Bl/6J male mice were injected with TNP-470 (30 mg/kg daily) or saline s.c. for 3 days. Then, mice were injected with IL-2 ($1.2 \times 10^6$ units/100 μl) or saline intraperitoneally (i.p.) three times a day for 5 days. At termination, mice were euthanized, and lungs were dissected, weighed, fixed, and processed for H&E staining.

**Tumor vascular permeability**

Female SCID mice (~8 weeks, ~20 g) were inoculated s.c. with $5 \times 10^6$ viable U87 glioblastoma, A2058 human melanoma, or BXPC3 pancreas adenocarcinoma cells. Female nu/nu mice were inoculated with $1 \times 10^6$ MCF-7 or MDA-MB-231 breast carcinoma cells in the mammary fat pad. C57Bl/6J were inoculated s.c. with $5 \times 10^6$ LLC cells. When tumors reached a volume of approximately 100 $mm^3$, mice were injected s.c. with free TNP-470 (as above) or caplostatin (30 mg/kg TNP-470-equivalent concentration) for 3 days, angiostatin (200 mg/kg s.c.) for 5 days, or saline (250 μl s.c.) for 5 days (n = 10). Evans blue dye was then injected i.v., and dye was extracted and assessed as above. Also, VPF/VEGF levels were measured in plasma and in tumors (n = 5 from each group). Tumors (n = 5 per group) were dissected, weighed, and bisected. Half of each tumor was placed in formalin, and half was analyzed for VPF/VEGF protein by ELISA (see below). Formalin-fixed tumors were processed for H&E sections as above and for CD31, SMA, and PCNA staining according to the manufacturer's instructions.

To determine the ability of TNP-470 to inhibit the permeability response induced by increasing doses of VPF/VEGF, 8-week-old C57Bl/6J mice were treated with TNP-470 (30 mg/kg/day s.c. for 3 days) or with saline. Evans blue (100 μl; 1%) was injected i.v., and after 10 min VPF/VEGF was injected intradermally at increasing concentrations (from $2.5 \times 10^{-5}$ to 250 ng/ml). Twenty minutes later, punch biopsies of flank skin from both sets of mice were taken and processed as above.

**ELISA assays for VPF/VEGF**

Blood drawn from tumor-bearing mice was centrifuged, and plasma was collected. Solid tumors were homogenized and resuspended in lysis buffer. In addition, tumor cells were plated at 500,000 cells per well (six-well plates), and conditioned medium from cells was collected 48 hr later. Levels of VPF/VEGF in plasma, tumors, and culture supernatants were determined in duplicate samples by ELISA (R&D Systems, MN).

**Cell proliferation assay**

HMVEC-d cells were plated at 15,000 cells/ml onto gelatinized 24-well culture plates in EBM-2 supplemented with 5% fetal bovine serum (FBS) and incubated for 24 hr (37°C; 5% $CO_2$). Medium was replaced with complete media (serum and growth factors; EGM-2 MV). U87 glioblastoma cells were plated at 5000 cells/ml in DMEM supplemented with 10% FBS and incubated for 24 hr (37°C; 5% $CO_2$). Medium was replaced with DMEM and 10% FBS. Both cell types were challenged with free or conjugated TNP-470 (0.01 pg/ml to 1 mg/ml TNP-470-equivalent concentration). Control cells were grown with or without growth factors. Both cell types were incubated for 72 hr, followed by trypsinization and resuspension in Hematall (Fisher Scientific, Pittsburgh, PA), and counted in a Coulter counter.

**Cell migration assay**

Cell migration was performed as previously described (Short et al., 2005) with the following modifications: suspended HMVEC-d were treated with free or conjugated TNP-470 at equivalent concentrations of 1 ng/ml, and cells were added to the upper chamber of the transwell for a 2 hr incubation prior to migration to VEGF.

**VEGFR-2 phosphorylation**

Serum-starved (0.1% FBS in EBM-2 media for 24 hr) HMVEC-d or HUVEC were treated with 5 ng/ml TNP-470 and caplostatin at 37°C for 2 hr and then stimulated with 10 ng/ml of VEGF for 5 min. Stimulation was stopped by adding cold PBS. Cells were lysed with cold precipitation buffer (20 mM Tris-HCl [pH 7.5], 0.15 M NaCl, 1% Triton X-100, 1 mM PMSF, 1 mM $Na_3VO_4$, 1 mM EGTA, 1 μg/ml leupeptin, 0.5% aprotinin, and 2 μg/ml pepstatin A). Lysate protein (500 μg) was incubated with 1 μg of antibody against VEGFR-2 for 2 hr, then with 50 μl of protein A-conjugated agarose beads at 4°C for 3–4 hr. After the beads were washed with precipitation buffer, immunoprecipitates were resuspended in 2× SDS sample buffer for Western blot analysis with an antibody against phosphorylated tyrosine (*pTyr*).

**RhoA activation assay**

pGST-TRBD bacteria were grown and induced with isopropyl-thiogalactoside. The bacterial suspensions were divided into 50 ml aliquots and then harvested and frozen at –80°C. To prepare the GST-TRBD beads, each aliquot of frozen bacteria was resuspended in 2 ml of cold PBS, and then 20 μl of 1 M dithiothreitol (DTT), 20 μl of 0.2 M PMSF, and 40 μl of 50 mg/ml lysozyme were added. The sample was incubated on ice for 30 min. Next, 225 μl of 10% Triton X-100, 22.5 μl of 1 M $MgCl_2$, and 22.5 μl of 2000 KU/ml DNase were added, and the sample was incubated on ice for another 30 min. The supernatant was collected and incubated with 100 μl glutathione-coupled Sepharose 4B beads (Pharmacia Biotech) at 4°C for 45 min. The beads were then washed with bead-washing buffer (PBS with 10 mM DTT and 1% Triton X-100) and resuspended in the same buffer to give a 50% bead slurry.

HMVEC-d cells serum-starved for 24 hr were treated with 5 ng/ml TNP-470 at 37°C for 2 hr and then stimulated with 10 ng/ml of VEGF, PAF (10 nM), or histamine (100 mM) for 5 min. Stimulation was stopped by adding cold PBS. Cells were lysed with lysis buffer (150 mM NaCl, 0.8 mM $MgCl_2$, 5 mM EGTA, 1% IGEPAL, 50 mM HEPES [pH 7.5], 1 mM PMSF, 10 μg/ml leupeptin, and 10 μg/ml aprotinin). The supernatant was isolated and incubated with 50 μl of GST-TRBD beads at 4°C for 45 min. Protein bound to beads was washed with AP wash buffer (50 mM Tris-HCl [pH 7.2], 1% Triton X-100, 150 mM NaCl, 10 mM $MgCl_2$, 1 mM PMSF, 10 μg/ml leupeptin, and 10 μg/ml aprotinin) and analyzed by SDS-PAGE with an antibody against RhoA (Santa Cruz Biotechnology, CA).

**Phosphorylation of MAPK**

Serum-starved HMVEC-d were treated with 5 ng/ml TNP-470 at 37°C for 2 hr and then stimulated with 10 ng/ml of VEGF for 5 min. Stimulation was

stopped by adding cold PBS. Cells were lysed with cold precipitation buffer. Cellular extracts (20 μg) were immunoblotted with an antibody against phosphorylated MAPK (p-MAPK) (Cell Signaling Technology Inc.). The blot was stripped and reprobed with an antibody against MAPK to confirm equal protein loading.

**$Ca^{2+}$ assays**

Serum-starved confluent HMVEC-d were detached with 4 ml of collagenase solution (0.2 mg/ml collagenase, 0.2 mg/ml soybean trypsin inhibitor, 1 mg/ml BSA, and 2 mM EDTA in PBS) at 37°C for 30 min on a 10 cm dish. Cells were centrifuged, and pellets were washed with 2 ml of $Ca^{2+}$ buffer (5 mM KCl, 140 mM NaCl, 1 mM $CaCl_2$, 1 mM $MgCl_2$, 5.6 mM glucose, 0.1% BSA, 0.25 mM sulfinpyrazone, and 10 mM HEPES [pH 7.5]) and then resuspended in 2 ml of the same buffer containing 5 ng/ml TNP-470. The cells were incubated at 37°C for 2 hr in suspension. During the last 30 min of incubation, 1 μg/ml Fura-2-AM (acetoxymethyl ester derivative of Fura 2) and 0.02% pluronic F-127 were added to the suspension. Cells ($10^6$) were collected and resuspended in 2 ml $Ca^{2+}$ buffer for VPF/VEGF (10 ng/ml), PAF (20 nM), or histamine (100 mM) stimulation, while the tubes were rocked. Intracellular $Ca^{2+}$ concentrations were measured with the Delta-Scan Illumination System (Photon Technology International Inc.) using Felix software.

**Acknowledgments**

We thank the Fulbright and the Rothschild Foundations (R.S.-F.), the National Institutes of Health (NIH) (research grant R01 CA064481 to R.S.-F. and J.F.), and the Breast Cancer Research Foundation for their financial support. This work is also partly supported by NIH research grants P01 CA45548 and R01 CA37395 (J.F.) and HL70567 and HL072178 (D.M.). The excellent technical assistance of Amy E. Birsner, Rachel W. Winter, and Ludmila M. Dobesova-Flores is acknowledged. We thank Kristin Gullage for photography and graphic art. We thank Shay Soker, Akiko Mammoto, and Sui Huang for useful discussions and Steven A. Rosenberg for the generous gift of IL-2.

Received: February 9, 2004
Revised: September 16, 2004
Accepted: February 15, 2005
Published: March 14, 2005

**References**

Abe, J., Zhou, W., Takuwa, N., Taguchi, J., Kurokawa, K., Kumada, M., and Takuwa, Y. (1994). A fumagillin derivative angiogenesis inhibitor, AGM-1470, inhibits activation of cyclin-dependent kinases and phosphorylation of retinoblastoma gene product but not protein tyrosyl phosphorylation or protooncogene expression in vascular endothelial cells. Cancer Res. *54*, 3407–3412.

Aoyagi, M., Arvai, A.S., Tainer, J.A., and Getzoff, E.D. (2003). Structural basis for endothelial nitric oxide synthase binding to calmodulin. EMBO J. *22*, 766–775.

Aramoto, H., Breslin, J.W., Pappas, P.J., Hobson, R.W., II, and Duran, W.N. (2004). Vascular endothelial growth factor stimulates differential signaling pathways in in vivo microcirculation. Am. J. Physiol. Heart Circ. Physiol. *287*, H1590–H1598.

Aspenstrom, P. (1999). Effectors for the Rho GTPases. Curr. Opin. Cell Biol. *11*, 95–102.

Berthiaume, Y., Boiteau, P., Fick, G., Kloiber, R., Sinclair, G.D., Fong, C., Poon, M.C., and Lafreniere, R. (1995). Pulmonary edema during IL-2 therapy: combined effect of increased permeability and hydrostatic pressure. Am. J. Respir. Crit. Care Med. *152*, 329–335.

Breslin, J.W., and Yuan, S.Y. (2004). Involvement of RhoA and Rho kinase in neutrophil-stimulated endothelial hyperpermeability. Am. J. Physiol. Heart Circ. Physiol. *286*, H1057–H1062.

Brock, T.A., Dvorak, H.F., and Senger, D.R. (1991). Tumor-secreted vascular permeability factor increases cytosolic Ca2+ and von Willebrand factor release in human endothelial cells. Am. J. Pathol. *138*, 213–221.

Brown, L.F., Dezube, B.J., Tognazzi, K., Dvorak, H.F., and Yancopoulos, G.D. (2000). Expression of Tie1, Tie2, and angiopoietins 1, 2, and 4 in Kaposi's sarcoma and cutaneous angiosarcoma. Am. J. Pathol. *156*, 2179–2183.

Carmeliet, P., and Collen, D. (2000). Molecular basis of angiogenesis. Role of VEGF and VE-cadherin. Ann. N Y Acad. Sci. *902*, 249–262.

Claesson-Welsh, L. (2003). Signal transduction by vascular endothelial growth factor receptors. Biochem. Soc. Trans. *31*, 20–24.

Claffey, K.P., Brown, L.F., del Aguila, L.F., Tognazzi, K., Yeo, K.T., Manseau, E.J., and Dvorak, H.F. (1996). Expression of vascular permeability factor/vascular endothelial growth factor by melanoma cells increases tumor growth, angiogenesis, and experimental metastasis. Cancer Res. *56*, 172–181.

Colvin, R.B., and Dvorak, H.F. (1975). Role of the clotting system in cell-mediated hypersensitivity. II. Kinetics of fibrinogen/fibrin accumulation and vascular permeability changes in tuberculin and cutaneous basophil hypersensitivity reactions. J. Immunol. *114*, 377–387.

Dvorak, H.F. (2002). Vascular permeability factor/vascular endothelial growth factor: a critical cytokine in tumor angiogenesis and a potential target for diagnosis and therapy. J. Clin. Oncol. *20*, 4368–4380.

Dvorak, A.M., Lett-Brown, M.A., Thueson, D.O., Pyne, K., Raghuprasad, P.K., Galli, S.J., and Grant, J.A. (1984). Histamine-releasing activity (HRA). III. HRA induces human basophil histamine release by provoking noncytotoxic granule exocytosis. Clin. Immunol. Immunopathol. *32*, 142–150.

Dvorak, A.M., Kohn, S., Morgan, E.S., Fox, P., Nagy, J.A., and Dvorak, H.F. (1996). The vesiculo-vacuolar organelle (VVO): a distinct endothelial cell structure that provides a transcellular pathway for macromolecular extravasation. J. Leukoc. Biol. *59*, 100–115.

Feng, D., Nagy, J.A., Hipp, J., Dvorak, H.F., and Dvorak, A.M. (1996). Vesiculo-vacuolar organelles and the regulation of venule permeability to macromolecules by vascular permeability factor, histamine, and serotonin. J. Exp. Med. *183*, 1981–1986.

Feng, D., Nagy, J.A., Dvorak, A.M., and Dvorak, H.F. (2000). Different pathways of macromolecule extravasation from hyperpermeable tumor vessels. Microvasc. Res. *59*, 24–37.

Feng, D., Nagy, J.A., Dvorak, H.F., and Dvorak, A.M. (2002). Ultrastructural studies define soluble macromolecular, particulate, and cellular transendothelial cell pathways in venules, lymphatic vessels, and tumor-associated microvessels in man and animals. Microsc. Res. Tech. *57*, 289–326.

Ferrara, N., and Henzel, W.J. (1989). Pituitary follicular cells secrete a novel heparin-binding growth factor specific for vascular endothelial cells. Biochem. Biophys. Res. Commun. *161*, 851–858.

Folkman, J., and Kalluri, R. (2003). Tumor angiogenesis. In Cancer Medicine, D.W. Kufe, R.E. Pollock, R.R. Weichselbaum, R.C.J. Bast, T.S. Gansler, J.F. Holland, and E.I. Frei, eds. (Hamilton, Ontario, Canada: B.C. Decker Inc.), pp. 161–194.

Folkman, J., Haudenschild, C.C., and Zetter, B.R. (1979). Long-term culture of capillary endothelial cells. Proc. Natl. Acad. Sci. USA *76*, 5217–5221.

Fukumura, D., Gohongi, T., Kadambi, A., Izumi, Y., Ang, J., Yun, C.O., Buerk, D.G., Huang, P.L., and Jain, R.K. (2001). Predominant role of endothelial nitric oxide synthase in vascular endothelial growth factor-induced angiogenesis and vascular permeability. Proc. Natl. Acad. Sci. USA *98*, 2604–2609.

Gad, S.C., Dunn, B.J., Dobbs, D.W., Reilly, C., and Walsh, R.D. (1986). Development and validation of an alternative dermal sensitization test: the mouse ear swelling test (MEST). Toxicol. Appl. Pharmacol. *84*, 93–114.

Gratton, J.P., Lin, M.I., Yu, J., Weiss, E.D., Jiang, Z.L., Fairchild, T.A., Iwakiri, Y., Groszmann, R., Claffey, K.P., Cheng, Y.C., and Sessa, W.C. (2003). Selective inhibition of tumor microvascular permeability by cavtratin blocks tumor progression in mice. Cancer Cell *4*, 31–39.

Griffith, E.C., Su, Z., Turk, B.E., Chen, S., Chang, Y.H., Wu, Z., Biemann, K., and Liu, J.O. (1997). Methionine aminopeptidase (type 2) is the common target for angiogenesis inhibitors AGM-1470 and ovalicin. Chem. Biol. *4*, 461–471.

Hall, A. (1998). Rho GTPases and the actin cytoskeleton. Science *279*, 509–514.

Hopkins, A.M., Walsh, S.V., Verkade, P., Boquet, P., and Nusrat, A. (2003). Constitutive activation of Rho proteins by CNF-1 influences tight junction structure and epithelial barrier function. J. Cell Sci. *116*, 725–742.

Ingber, D.E. (2002). Mechanical signaling and the cellular response to extracellular matrix in angiogenesis and cardiovascular physiology. Circ. Res. *91*, 877–887.

Ingber, D., Fujita, T., Kishimoto, S., Sudo, K., Kanamaru, T., Brem, H., and Folkman, J. (1990). Synthetic analogues of fumagillin that inhibit angiogenesis and suppress tumour growth. Nature *348*, 555–557.

Kerbel, R., and Folkman, J. (2002). Clinical translation of angiogenesis inhibitors. Nat. Rev. Cancer *2*, 727–739.

Koch, A.E., Harlow, L.A., Haines, G.K., Amento, E.P., Unemori, E.N., Wong, W.L., Pope, R.M., and Ferrara, N. (1994). Vascular endothelial growth factor. A cytokine modulating endothelial function in rheumatoid arthritis. J. Immunol. *152*, 4149–4156.

Kragh, M., Spang-Thomsen, M., and Kristjansen, P.E. (1999). Time until initiation of tumor growth is an effective measure of the anti-angiogenic effect of TNP-470 on human glioblastoma in nude mice. Oncol. Rep. *6*, 759–762.

Matsumoto, T., and Claesson-Welsh, L. (2001). VEGF receptor signal transduction. Sci. STKE *2001*, RE21.

Mauriz, J.L., Linares, P., Macias, R.I., Jorquera, F., Honrado, E., Olcoz, J.L., Gonzalez, P., and Gonzalez-Gallego, J. (2003). TNP-470 inhibits oxidative stress, nitric oxide production and nuclear factor κB activation in a rat model of hepatocellular carcinoma. Free Radic. Res. *37*, 841–848.

McLeskey, S.W., Zhang, L., Trock, B.J., Kharbanda, S., Liu, Y., Gottardis, M.M., Lippman, M.E., and Kern, F.G. (1996). Effects of AGM-1470 and pentosan polysulphate on tumorigenicity and metastasis of FGF-transfected MCF-7 cells. Br. J. Cancer *73*, 1053–1062.

Mehta, D., Ahmmed, G.U., Paria, B., Holinstat, M., Voyno-Yasenetskaya, T., Tiruppathi, C., Minshall, R.D., and Malik, A.B. (2003). RhoA interaction with inositol 1,4,5-triphosphate receptor and transient receptor potential channel-1 regulates Ca2+ entry. Role in signaling increased endothelial permeability. J. Biol. Chem. *278*, 33492–33500. Published online May 22, 2003. 10.1074/jbc.M302401200

Miles, A.A., and Miles, E.M. (1952). Vascular reactions to histamine, histamine liberators or leukotoxins in the skin of the guinea pig. J. Physiol. *118*, 228–257.

Milkowski, D.M., and Weiss, R.A. (1999). TNP-470. In Antiangiogenic Agents in Cancer Therapy, T.A. Teicher, ed. (Totowa, NJ: Human Press Inc.), pp. 385–398.

Neufeld, G., Cohen, T., Gengrinovitch, S., and Poltorak, Z. (1999). Vascular endothelial growth factor (VEGF) and its receptors. FASEB J. *13*, 9–22.

Ohnishi, T., Sher, P.B., Posner, J.B., and Shapiro, W.R. (1990). Capillary permeability factor secreted by malignant brain tumor. Role in peritumoral brain edema and possible mechanism for anti-edema effect of glucocorticoids. J. Neurosurg. *72*, 245–251.

O'Reilly, M.S., Holmgren, L., Shing, Y., Chen, C., Rosenthal, R.A., Moses, M., Lane, W.S., Cao, Y., Sage, E.H., and Folkman, J. (1994). Angiostatin: a novel angiogenesis inhibitor that mediates the suppression of metastases by a Lewis lung carcinoma. Cell *79*, 315–328.

Ren, X.D., Kiosses, W.B., and Schwartz, M.A. (1999). Regulation of the small GTP-binding protein Rho by cell adhesion and the cytoskeleton. EMBO J. *18*, 578–585.

Satchi-Fainaro, R., Puder, M., Davies, J.W., Tran, H.T., Sampson, D.A., Greene, A.K., Corfas, G., and Folkman, J. (2004). Targeting angiogenesis with a conjugate of HPMA copolymer and TNP-470. Nat. Med. *10*, 255–261.

Senger, D.R., Galli, S.J., Dvorak, A.M., Perruzzi, C.A., Harvey, V.S., and Dvorak, H.F. (1983). Tumor cells secrete a vascular permeability factor that promotes accumulation of ascites fluid. Science *219*, 983–985.

Short, S.M., Derrien, A., Narsimhan, R.P., Lawler, J., Ingber, D., and Zetter, B.R. (2005). Inhibition of endothelial cell migration by thrombospondin-1 type-1 repeats is mediated by β1 integrins. J. Cell Biol. *168*, 643–653.

Streit, M., Velasco, P., Riccardi, L., Spencer, L., Brown, L.F., Janes, L., Lange-Asschenfeldt, B., Yano, K., Hawighorst, T., Iruela-Arispe, L., and Detmar, M. (2000). Thrombospondin-1 suppresses wound healing and granulation tissue formation in the skin of transgenic mice. EMBO J. *19*, 3272–3282.

Takamiya, Y., Brem, H., Ojeifo, J., Mineta, T., and Martuza, R.L. (1994). AGM-1470 inhibits the growth of human glioblastoma cells in vitro and in vivo. Neurosurgery *34*, 869–875.

Tjin Tham Sjin, R.M., Satchi-Fainaro, R., Birsner, A.E., Ramanujam, V.M.S., Folkman, J., and Javaherian, K. (2005). A 27 amino acid synthetic peptide corresponding to the N-terminal zinc binding domain of endostatin is responsible for its anti-tumor activity. Cancer Res., in press.

Yamaoka, M., Yamamoto, T., Ikeyama, S., Sudo, K., and Fujita, T. (1993). Angiogenesis inhibitor TNP-470 (AGM-1470) potently inhibits the tumor growth of hormone-independent human breast and prostate carcinoma cell lines. Cancer Res. *53*, 5233–5236.

Zeng, H., Zhao, D., and Mukhopadhyay, D. (2002). KDR stimulates endothelial cell migration through heterotrimeric G protein Gq/11-mediated activation of a small GTPase RhoA. J. Biol. Chem. *277*, 46791–46798.